Mon. Not. R. Astron. Soc. **000**, 000–000 (0000) Printed 19 May 2010 (MN LATEX style file v2.2)

Galaxy Pairs in the Sloan Digital Sky Survey - II: The Effect of Environment on Interactions.

Sara L. Ellison[1], David R. Patton[2], Luc Simard[3], Alan W. McConnachie[3], Ivan K. Baldry[4], J. Trevor Mendel[1]

[1] *Department of Physics and Astronomy, University of Victoria, Victoria, British Columbia, V8P 1A1, Canada.*
[2] *Department of Physics & Astronomy, Trent University, 1600 West Bank Drive, Peterborough, Ontario, K9J 7B8, Canada.*
[3] *National Research Council of Canada, Herzberg Institute of Astrophysics, 5071 West Saanich Road, Victoria, British Columbia, V9E 2E7, Canada*
[4] *Astrophysics Research Institute, Liverpool John Moores University, Twelve Quays House, Egerton Wharf, Birkenhead, CH41 1LD, UK.*

arXiv:1002.4418v2 [astro-ph.CO] 17 May 2010

19 May 2010

ABSTRACT

We use a sample of close galaxy pairs selected from the Sloan Digital Sky Survey Data Release 4 (SDSS DR4) to investigate in what environments galaxy mergers occur and how the results of these mergers depend on differences in local galaxy density. The galaxies are quantified morphologically using two-dimensional bulge-plus-disk decompositions and compared to a control sample matched in stellar mass, redshift and local projected density. Lower density environments have fractionally more galaxy pairs with small projected separations (r_p) and relative velocities (Δv), but even high density environments contain significant populations of pairs with parameters that should be conducive to interactions. The connection between environment and Δv also implies that the velocity selection of a pairs sample affects (biases) the environment from which the pairs are selected. Metrics of asymmetry and colour are used to identify merger activity and triggered star formation. The location of star formation is inferred by distinguishing bulge and disk colours and calculating bulge fractions from the SDSS images. Galaxies in the lowest density environments show the largest changes in star formation rate, asymmetry and bulge-total fractions at small separations, accompanied by bluer bulge colours. At the highest local densities, the only galaxy property to show an enhancement in the closest pairs is asymmetry. We interpret these results as evidence that whilst interactions (leading to tidal distortions) occur at all densities, triggered star formation is seen only in low-to-intermediate density environments. We suggest that this is likely due to the typically higher gas fractions of galaxies in low density environments. Finally, by cross-correlating our sample of galaxy pairs with a cluster catalogue, we investigate the dependence of interactions on clustercentric distance. It is found that for close pairs the fraction of asymmetric galaxies is highest in the cluster centres.

Key words: galaxies: evolution, galaxies: bulges, galaxies: interactions

1 INTRODUCTION

Galaxies in high density environments have been shown to be unequivocally different to their isolated counterparts. From the discovery of the morphology-density relation (e.g. Dressler 1980; Postman & Geller 1984), the colours, morphologies and mean star formation rates of galaxies all clearly depend on their local environment (e.g Kauffmann et al. 2004; Balogh et al. 2004; Baldry et al. 2006; Weinmann et al. 2006; Park et al 2007; Skibba et al. 2009; Bamford et al. 2009 and references therein). Disentangling the process(es) that drive these environmental dependences, the scales on which environment matters and identifying which are the primary changes in galaxy properties is a major theme in contemporary astrophysics (e.g. Blanton & Berlind 2007; Park & Choi 2009; Deng et al. 2009).

In this paper, we tackle the specific issue of tidal interactions between galaxies and how gravitationally induced effects, such as triggered star formation and morphological transformation, depend on the larger scale environment. It has been well known for many years that galaxy-galaxy interactions can trigger star formation, e.g. Kennicutt et al., (1987); Barton, Geller & Kenyon (2000); Lambas et al (2003); Alonso et al. (2004); Nikolic, Cullen & Alexander (2004). The enhanced star formation that accompanies galaxy-galaxy interactions appears to be relatively modest, around a factor of two on average, and many close pairs have 'normal' star formation rates (e.g. Barton et al. 2000; Bergvall et al. 2003; Lin et al. 2007; Darg et al. 2010; Knapen & James 2009; Robaina et al. 2009). However, the efficiency with which star formation is triggered depends strongly on not only internal, but also the relative,

macroscopic properties of galaxies in interactions. Major galaxy-galaxy interactions (where the ratio of galaxy masses or luminosities is close to unity) trigger the strongest star formation (Woods, Geller & Barton 2006; Ellison et al. 2008). In minor (unequal mass) pairs, the lower mass galaxy appears to be more affected by triggered star formation than the more massive counterpart (Donzelli & Pastoriza 1997; Woods & Geller 2007; Ellison et al. 2008; Li et al. 2008), as predicted by simulations (Bekki, Shioya & Whiting 2006; Cox et al. 2008). Simulations also predict that the orientation and relative rotation directions can dramatically affect the efficiency of a starburst, much more so than simply the presence of an adequate gas supply (Di Matteo et al. 2007; Cox et al. 2008). The efficiency may also increase at higher redshifts (e.g. Bridge et al. 2007) where some of the most luminous galaxies in the UV are seen to have close companions and exhibit signs of interactions (Basu-Zych et al. 2009).

The triggered star formation is expected to occur in the nuclear regions of the galaxy as gas loses angular momentum during the interaction, modulated by the presence of a bulge (Mihos & Hernquist 1994, 1996; Cox et al. 2008). This prediction is supported observationally by lower nuclear metallicities (Kewley et al. 2006; Ellison et al. 2008), blue central colours and larger Hα equivalent widths (Barton et al. 2003; Bergvall et al. 2003; Kannappan et al. 2004) and higher concentration indices and bulge fractions (Nikolic et al. 2004; Li et al. 2008; Perez et al. 2009b) in close pairs. Recently, Soto & Martin (2009) have added further evidence to this scenario from the detection of age gradients in Ultra Luminous Infra-Red Galaxies (ULIRGs) that are consistent with gas removal from the outer regions to fuel continuous star formation in the centres. In addition to a population of very blue galaxies, and examples of highly efficient star formation, close pairs also appear to have a notable red population (Alonso et al. 2006; Darg et al. 2010; Perez et al. 2009b). Triggered star formation in mergers, although prevalent in late-type galaxies, is not significant in early-type pairs, probably due to their low gas fractions (Luo, Shu & Huang 2007; Park & Choi 2009; Darg et al. 2010; Rogers et al. 2009).

A number of previous works have assessed the role of local environment on galaxy-galaxy interactions. Lambas et al. (2003) and Alonso et al. (2004) studied 2-degree field (2dF) pairs in the field and in groups respectively. It was found that in groups, enhanced star formation required smaller separations than in the field. Alonso et al. (2006) extended the 2dF analysis to include pairs in the Sloan Digital Sky Survey (SDSS) and compared the birth rate parameter (*b*, proportional to the specific star formation rate) in low, intermediate and high density environments, using the 5th nearest neighbour (Σ_5) as a density estimator for galaxies in the SDSS. Enhanced star formation was seen in wider separation pairs for lower Σ_5. Although enhanced star formation and bluer colours were found most significantly for pairs in the lowest density environments, the results may be biased by the fact that Alonso et al. (2006) did not match their control sample equally in Σ_5 (Perez et al. 2009a). Perez et al. (2009b) have recently improved upon this analysis, by constructing samples of pairs and control galaxies matched in stellar and dark matter halo mass, redshift and Σ_5. It was found that although pairs in the lowest density environments have the highest absolute fraction of star forming galaxies, pairs with projected separations $r_p < 20$ kpc have approximately twice the fraction of high *b* galaxies compared to the control, regardless of local density. However, Perez et al. (2009b) report that the colour and concentration distributions of the pairs and control differ most at intermediate densities (but see Patton et al in prep and Simard et al. in prep. for caveats on the use of SDSS photometry in crowded environments). Therefore, although the enhanced star formation in low density environments is likely the cause of a tail of very blue galaxies, the effect on the overall colour distribution is minor. Perez et al. (2009b) suggested that intermediate density environments, perhaps synonymous with groups, are the most important environment for galaxy interactions and mergers.

We are investigating the effects of environment on galaxy evolution by looking at galaxies in a range of environments; clusters (Ellison et al. 2009), compact groups (McConnachie et al. 2008, 2009; Brasseur et al. 2008) and pairs, of which this is the second paper in the series. In Paper I (Ellison et al. 2008) we focussed on a sample with strong emission lines to investigate the effect of galaxy interactions on the mass-metallicity relation and fraction of active galactic nuclei. In two forthcoming papers, Patton et al. (in preparation) use a larger sample to study the global colours of galaxy pairs, and Simard et al. (in preparation) examine the detailed morphological properties of pairs. In this paper we re-visit the issue of mergers and triggered star formation as a function of environment by considering the effect of both projected density and cluster membership on the same sample of close pairs. This is important in order to disentangle different physical processes and dependences. For example, the star formation rates (e.g. Gomez et al. 2003; Lewis et al. 2002) and mass-metallicity relation (Ellison et al. 2009) of galaxies are apparently dictated more by local density than cluster membership, possibly because these effects are driven by galaxy-galaxy interactions. On the other hand, the fraction of post-starburst galaxies is more dependent on cluster or group membership (e.g. Poggianti et al. 2009), indicating that ram pressure stripping may be important (Ma & Ebeling 2009).

The layout of the paper is as follows. In Section 2 we describe the selection of our pairs sample and the construction of a matched control sample. A properly designed control sample is essential for disentangling the effects of galaxy-galaxy interactions from biases in the pairs selection, such as projection effects (e.g. Perez et al. 2009a) or photometric errors. In Section 3 the dependence of pairwise properties as a function of environment, as defined by a 2-dimensional projected density, are investigated. The colours, asymmetry and bulge fractions of the close pairs sample are then analysed as a function of projected separation and environment. The importance of cluster membership is investigated in Section 4.

We adopt a concordance cosmology of $\Omega_\Lambda = 0.7$, $\Omega_M = 0.3$ and $H_0 = 70$ km/s/Mpc.

2 SAMPLE SELECTION AND CHARACTERIZATION

The galaxy sample used in this work is selected from the SDSS Data Release (DR) 4 and uses similar criteria to those defined by Patton et al. (in prep.). We briefly review the salient selection criteria here, highlighting the distinction with the other papers in this series (Ellison et al. 2008; Patton et al. in prep; Simard et al. in prep.).

(i) Extinction corrected Petrosian magnitudes must be in the range $14.5 < r \leqslant 17.77$. Objects must be classified as galaxies from SDSS imaging and in the SDSS spectroscopic catalogue (*SpecPhoto.SpecClass=2* and *SpecPhoto.Type=3*).

(ii) Galaxies must be unique spectroscopic objects and the SDSS SpecObjAll parameter which measures the redshift confidence must have a value exceeding $zconf > 0.7$.

(iii) In contrast to the sample of Patton et al. (in prep.), we impose an upper redshift cut-off of $z = 0.1$, because cluster mem-

bership (in this work, we use the catalogue of von der Linden et al. 2007) and local densities have only been determined up to this distance.

(iv) Due to incompleteness in the SDSS spectroscopic sample incurred by a minimum fibre separation of 55 arcsecs, wide separation pairs are preferentially selected at $z < 0.08$ (see Figure 1 of Ellison et al. 2008). Ellison et al. (2008) therefore removed a fraction of the wide separation pairs to yield a sample unbiased in the redshift-projected separation plane. Without this culling procedure, the distribution of mass ratios is slightly more peaked around equal mass pairs, due to the preferential omission of pairs with highly disparate masses. This effect is well-known and attributed to the loss of dynamical range in magnitude limited samples (e.g., Patton & Atfield 2008). The same culling procedure is used here.

(v) The morphology of the galaxy must be successfully modelled as a bulge plus disk in the *g*- and *r*-band with the Galaxy Image 2D (GIM2D) software (see Section 2.1). The percentage of fits that failed is small – 0.17%. The details of the GIM2D software are documented in Simard et al. (2002). Unless otherwise stated, we use the rest frame magnitudes derived from GIM2D with k-corrections applied from Blanton & Roweis (2007).

(vi) Relative stellar masses of the two galaxies in a pair (taken from Kauffmann et al. 2003) must be within a factor of 10. See Ellison et al. (2008) for a discussion of selection based on relative flux rather than mass.

(vii) The projected separation between a galaxy and its companion must be within $r_p < 80\ h_{70}^{-1}$ kpc.

(viii) The rest-frame velocity difference of a galaxy pair must be $\Delta v < 500$ km s^{-1}.

These criteria result in a sample of 5784 galaxies with a close companion. A control sample is constructed by selecting galaxies without close companions that fulfill the first five of the above criteria and are matched in redshift, stellar mass and environment, as defined by

$$\log \Sigma = \frac{1}{2} \log\left(\frac{4}{\pi d_4^2}\right) + \frac{1}{2} \log\left(\frac{5}{\pi d_5^2}\right). \quad (1)$$

i.e. a projected galaxy density averaged from the distances to the 4th and 5th nearest neighbours within 1000 km s^{-1} (Baldry et al. 2006). We adopt the densities re-computed by Ellison et al. (2009) using a density-defining population with $M_r < -20.6$, which yields a volume-limited sample out to $z = 0.11$. To account for missing spectroscopic redshifts, $\log \Sigma$ is also calculated using photometric redshifts. The final value of $\log \Sigma$ is the average of the spectroscopic redshift value and the value calculated with the inclusion of photometric redshifts (see Baldry et al 2006 for further discussion). We note that the distances to the 4th and 5th nearest neighbours are large ($\gg 500\ h_{70}^{-1}$ kpc) compared to the separation of the galaxy pairs ($< 80\ h_{70}^{-1}$ kpc). For example, the median values of d_4 and d_5 are 1.4 and 1.8 Mpc respectively, more than an order of magnitude larger than the separation of the pairs themselves. The presence of a close companion therefore does not bias the use of Σ as a density indicator. The control sample is constructed by matching each pair galaxy in redshift, stellar mass and Σ with a galaxy with no close companion. After matching each of the 5784 pair galaxies, the Komogorov-Smirnov (KS) probability that the control sample is drawn from the same distribution of redshift, stellar mass and density is calculated. If all the probabilities are better than 30%, the matching procedure is considered successful and is repeated. Four control galaxies per pair galaxy were allocated before the KS probability dropped below the 30% tolerance level.

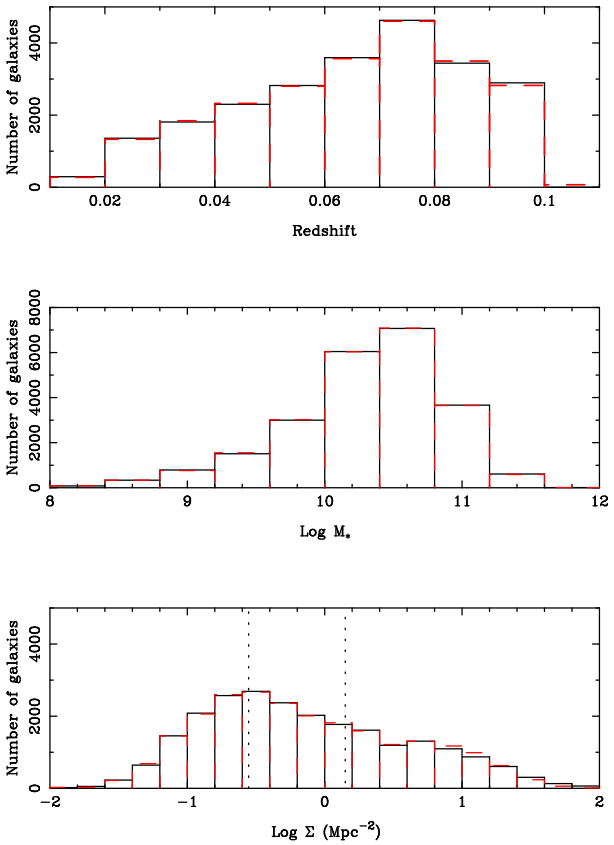

Figure 1. Physical properties of the galaxy pair sample. Dashed red histograms show the distributions of the control samples and solid lines represent the galaxies in close pairs. All of the black histograms have been scaled by a factor of four so that the total number of galaxies shown is the same as for the control sample. Vertical dashed lines in the lower panel indicate the boundaries between the three tertiles in projected density.

In Figure 1 we show the distribution of pair and control galaxy properties. Visually, it can be seen that the control and the pairs are well-matched in *z*, stellar mass and Σ. The KS probabilities that the pairs and control are drawn from the same parent population are 99.7% (redshift), 99.9% (stellar mass) and 63.3% (Σ). Also marked on Figure 1 are the values of Σ that correspond to equal thirds of the distribution (i.e. tertile boundaries). The corresponding values are $\log \Sigma = -0.55$ and 0.15. These are close to the boundaries defined by Perez et al. (2009b) for their low, intermediate and high density environments (as defined by the distance to the 5th nearest neighbour). In Figure 2 we show the pairwise galaxy properties for our sample: projected and angular separation, Δv and stellar mass ratio.

2.1 Morphological decomposition

GIM2D is used to re-derive all the galaxy photometry, as well as to determine morphological parameters. The software is described in detail by Simard et al. (2002). In the work presented here, we focus on the bulge-to-total (B/T) ratios and galaxy asymmetries. In brief, GIM2D fits a two component model (bulge plus disk) to each galaxy image, taking into account the image point spread function (PSF). The ratio of flux in the bulge relative to the total galaxy light yields the B/T ratio and can be derived separately in each bandpass. When multiple bands are fit, it is also possible to combine the

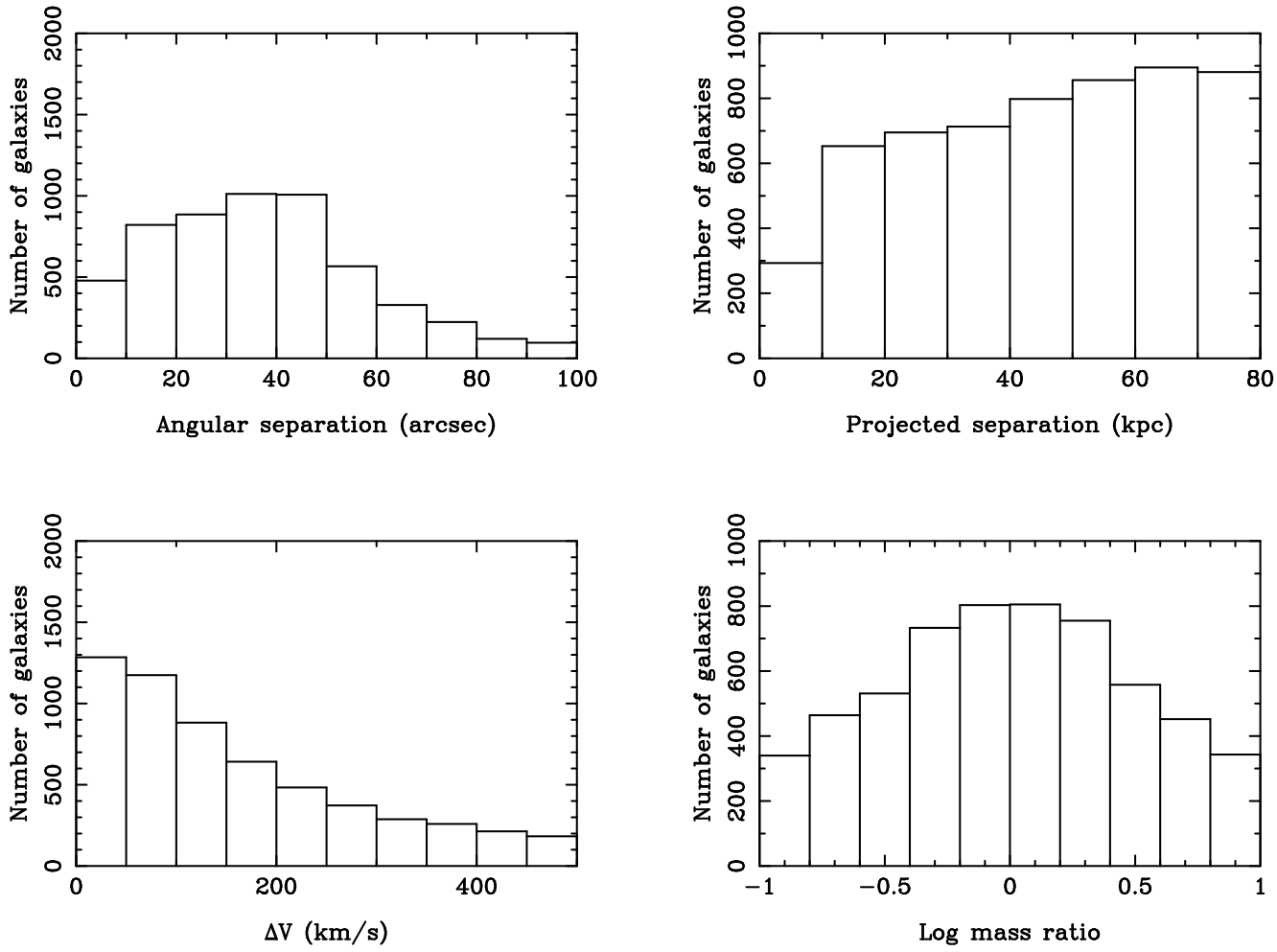

Figure 2. Pairwise properties of the overall galaxy pair sample.

component solutions to yield bulge and disk colours, in addition to integrated photometry. Bulge and disk absolute magnitudes in any given band are derived from

$$M_{\rm bulge} = M_{\rm galaxy} - 2.5\log(B/T) \quad (2)$$

$$M_{\rm disk} = M_{\rm galaxy} - 2.5\log(1 - B/T) \quad (3)$$

where $M_{\rm galaxy}$ is the total galaxy absolute magnitude and B/T is the bulge-to-total fraction (in the same band). Asymmetry can be quantified in many ways; we make use of the GIM2D parameter $R_T + R_A$. This metric involves subtracting the bulge plus disk model from both the original image and a 180-degree rotated version thereof. $R_T + R_A$ is the sum of the residuals in these subtracted images, normalized by the total (original) image flux.

When dealing with close pairs of galaxies, it is vital to be vigilent for the possible effects of crowding on the photometry and morphological decomposition. For example, Masjedi et al. (2006) found a dramatic increase in flux in object pairs at separations of < 3 arcsecs, but extending out as far as 20 arcseconds (see also McIntosh et al. 2008). We have carefully studied the residual images of GIM2D fits and find that the closest pairs often have poorly fitted backgrounds and inappropriate segmentation images from SDSS (Simard et al. in preparation). This problem manifests itself most dramatically in the scaling relation between disk size and luminosity where the close pairs show a strong excess of very large disks at a given luminosity (and consequently under-estimating the bulge fractions). We have made adjustments to the GIM2D fitting parameters to account for crowding issues in our close pairs sample. These include re-computing the local object backgrounds and fitting the bulge and disk models in the *g* and *r*-bands simultaneously. Full details of the fitting of the SDSS galaxies is given in Simard et al. (in preparation), which also presents a catalogue of the GIM2D parameters of ∼ 2.2 million galaxies in the SDSS spectroscopic sample with $r < 18$. The improved fitting not only removes the excessive presence of large disks, but also removes many of the extremely blue and red objects that had been found in previous pair samples. The integrated colours of our pairs sample is dealt with in a separate paper (Patton et al., in preparation).

3 THE ENVIRONMENT OF GALAXY PAIRS

In this section, we investigate how the local environment, as defined by Σ, affects the selection of galaxies with a close companion, and how such an environmental dependence influences their observed properties. Close galaxy pairs show increased star formation rates when their physical separations and relative velocities are small (e.g. Alonso et al. 2004, 2006). Moreover, Ellison et al. (2008) showed that star formation in galaxy pairs is more enhanced for more equal mass pairings than for unequal mass pairings, as

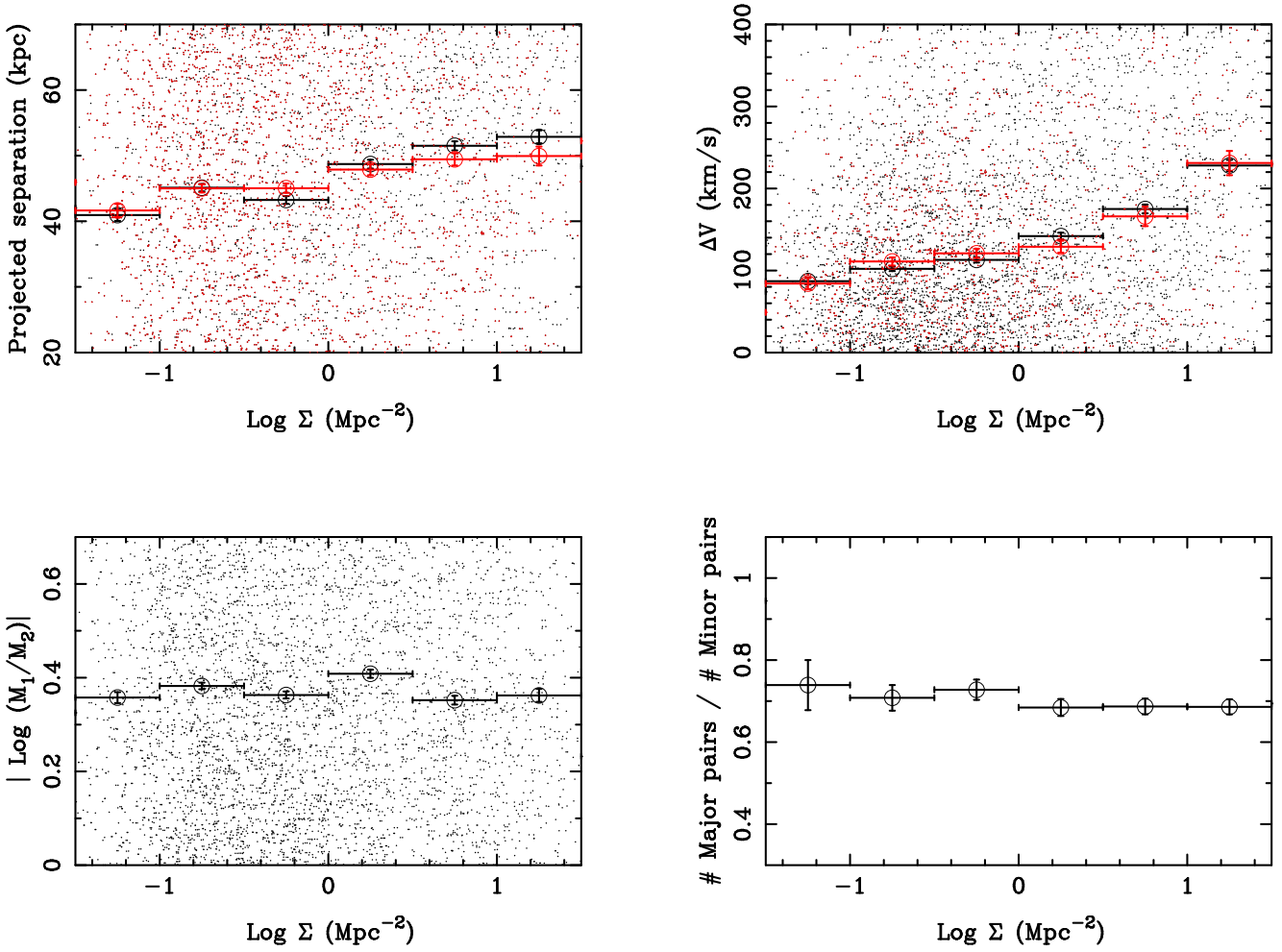

Figure 3. Pairwise properties as a function of projected galaxy density (environment), Σ. The individual galaxies are shown as small dots, the binned medians and error (RMS/$\sqrt{N}$) are shown with open circles. Red points indicate either pair galaxies with $r_p < 30\ h_{70}^{-1}$ kpc (upper right panel) or pair galaxies with $\Delta v < 200$ km s^{-1} (upper left panel).

predicted by simulations (e.g. Cox et al. 2008). It is therefore germane to investigate whether different environments host pairs whose physical properties are more conducive to galaxy-galaxy interactions.

3.1 Pairwise properties as a function of environment - where will mergers occur?

In Figure 3 the pairwise properties of our sample are shown as a function of Σ. For trends of Σ with r_p and ΔV, we consider both the full sample (black points) and only those galaxies in the closest pairs ($r_p < 30\ h_{70}^{-1}$ kpc, $\Delta v < 200$ km s^{-1}, red points). The mass ratio distributions are investigated with two different metrics - the median stellar mass ratio (the absolute value of the logarithm is used so that the primary and secondary counterparts of a given pair are counted in the same bin), and the ratio of major to minor pairs. A major pair is defined as having a ratio of stellar masses $0.5 < M_1/M_2 < 2$. Figure 3 shows that the median mass ratio of pairs and the fraction of major-to-minor pairs are independent of local environment. However, more dense environments become increasingly dominated by wider separation and high Δv pairs. Particularly noticable is the dominant population of $\Delta v < 200$ km s^{-1} pairs in environments with $-1 < \log\Sigma < 0$. Figure 4 demonstrates the same result in a different way. Histograms of projected separation, Δv and mass ratio are shown for the three Σ tertiles (with boundaries $\log\Sigma = -0.55, 0.15$, see Figure 1). The mass ratio histograms trace each other closely for the three environments, but the ΔV and projected separation histograms are significantly different. Low density environments ($\log\Sigma < -0.55$) are dominated by low velocity separation pairs, with only 7% exhibiting $\Delta v > 300$ km s^{-1}. In contrast, 30% of the high density ($\log\Sigma > 0.15$) have $\Delta v > 300$ km s^{-1}. The projected separation distributions are also skewed, although less dramatically. Low density environments have a slight excess of pairs with small separations ($r_p < 20\ h_{70}^{-1}$ kpc) and deficit of pairs with wide separations ($r_p > 50\ h_{70}^{-1}$ kpc), relative to the pairs in high density environments.

The corrollary of Figures 3 and 4 is two-fold. First, low density environments may be the most common sites for mergers, since they have a higher fraction of pairs with lower Δv and lower r_p. 34% of the lowest density tertile have $\Delta v < 200$ km s^{-1} and $r_p < 40\ h_{70}^{-1}$ kpc, compared to only 20% for the highest density tertile. Second, although a significant fraction of galaxy pairs may be found in dense environments (Barton et al. 2007; Perez et al. 2009b), a higher fraction of these pairs have large relative velocities which may hinder a final merger. Nonetheless, a significant fraction of galaxies even at high densities have low Δv and r_p, and yet galaxies

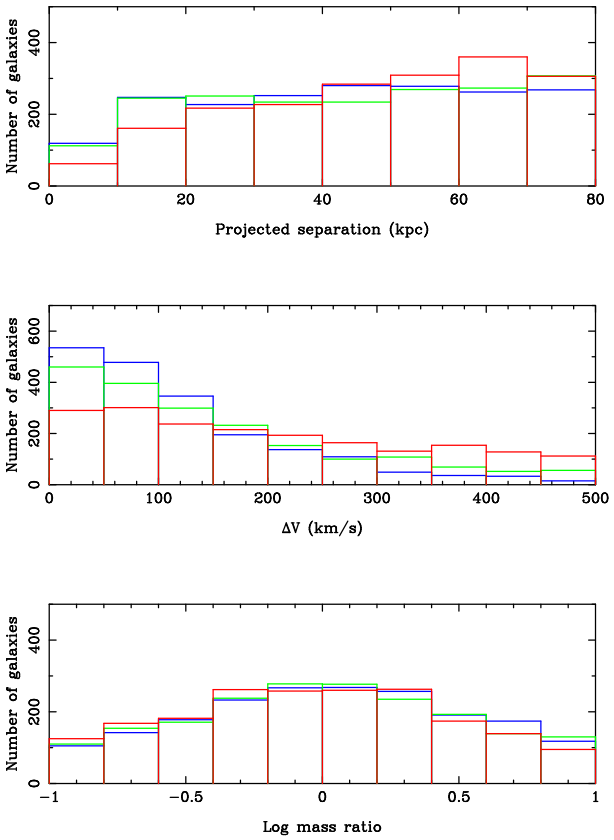

Figure 4. Histograms of pairwise properties for galaxies in high ($\log\Sigma > 0.15$, red), intermediate ($-0.55 < \log\Sigma < 0.15$, green) and low ($\log\Sigma < -0.55$, blue) density environments. Although the mass ratios of pairs is independent of environment (lower panel), lower local densities have a higher fraction of pairs with small Δv and smaller r_p.

in high density environments do not seem to exhibit much triggered star formation (Darg et al. 2010; Perez et al. 2009b). We return to this point in Section 3.2.

It is also noteworthy that the dependence of the distribution of Δv on environment means that relative velocity itself is a coarse proxy for local density. This is not surprising, given that more massive (high density) structures, such as clusters have larger velocity dispersion. This means that care must be taken when comparing different samples of galaxy pairs, since different tolerances of Δv will lead to a different mix of galaxy types. Pair samples with a lower Δv threshold will tend to include more later type galaxies, characterised with higher star formation rates and smaller bulges, on average. Moreover, relative velocities of 1000 km s^{-1} are possible at peri-galacticon and Patton et al. (in prep.) show that close pairs exhibit evidence of interaction even when $\Delta v \sim 500 - 1000$ km s^{-1}. The trends of star formation rate with Δv that have previously been shown in, e.g., Alonso et al. (2006), may therefore not be an indicator of the relative velocity required for an interaction, but may simply trace the change in galaxy population. However, the frequency of truly interacting pairs is likely to increase at smaller Δv, so that a cut-off in the range of a few hundred km s^{-1} is useful for minimizing contamination.

The weak dependence of r_p with Σ is a less intuitive effect to understand and we suggest that it may be caused by a number of contributing factors. At larger (projected) densities, contamination by (non-interacting) interlopers becomes more severe. Projection effects preferentially contribute at larger r_p and may therefore skew the median r_p to higher values at higher values of Σ (e.g. Perez et al. 2006). We show in the upper left panel of Figure 3 that this is a contributing factor by comparing the full pairs sample ($\Delta v < 500$ km s^{-1}, black points) with those whose relative velocity is only $\Delta v < 200$ km s^{-1} (red points). The lower velocity sample will contain fewer projected interlopers, and indeed the correlation between r_p and Σ is weaker in the $\Delta v < 200$ km s^{-1} pairs. Another contributing factor is a redshift bias, combined with fibre collisions. The high Σ sample has fewer lower redshift galaxies and proportionately more high redshift ones. This is due to both the limited volume sampling for rare high density structures at low z and the fact that galaxies in high density environments tend to be more luminous and can therefore be detected out to greater distances. For a given r_p, the angular separation on the sky is smaller at higher redshifts. Patton & Atfield (2008) have shown that the spectroscopic incompleteness of the SDSS steadily declines within the 55 arcsecond fibre collision radius, and drops sharply (by a factor of 2) within 10 arcseconds (15 h_{70}^{-1} kpc at $z = 0.08$). This will lead to a higher incompleteness at small physical separations for the higher density pairs. However, we emphasize that any dependence on Σ (such as redshift) is accounted for in our analysis by matching in the control sample.

The lack of dependence of mass ratio on environment indicates that the efficiency of triggered star formation in minor versus major pairs is unlikely to bias observations.

3.2 Star formation rates

It is well known that enhanced star formation is seen in close pairs of galaxies (e.g. Kennicutt et al., 1987; Barton, Geller & Kenyon 2000; Lambas et al 2003; Alonso et al. 2004; Nikolic, Cullen & Alexander 2004; Woods et al. 2006; Li et al. 2008; Ellison et al. 2008). Before investigating how the enhancement of specific star formation rate (SSFR) depends on environment, we first assess whether the pairs sample may systematically vary as a function of separation, introducing a dependence on r_p that is independent of interactions. The most important possible bias is that of stellar mass. In Figure 5 we show the mass of galaxies in pairs (and their matched control) as a function of separation. The top left panel shows that the full pairs sample is biased to slightly lower stellar masses in the inner most separation bin, relative to the rest of the sample. A more striking deviation is seen in the low density sample where pairs in the two smallest projected separation bins ($r_p < 30$ h_{70}^{-1} kpc) have median stellar masses that differ by approximately 0.1 dex from the median of the full sample. This is not due to small number statistics – there are ~ 230 galaxies in each bin. The control galaxy masses track the pair galaxies in a given bin because stellar mass is one of the quantities that is matched. Figure 5 highlights the importance of control sample matching and shows that it is the offset between the control and pairs *at a given separation* that reveals the presence of interaction-induced effects.

In Figure 6 the specific star formation rate for the pairs sample is shown as a function of projected separation for pairs whose $\Delta v < 200$ km s^{-1}. The star formation rates are total, aperture-corrected values from Brinchmann et al. (2004). The panels show the pairs in the full sample (upper left) and in the three Σ density tertiles. In each panel, the horizontal dashed line shows the median value for the control galaxies in the appropriate Σ sample. We also show the control values binned by projected separation, where the value of r_p is taken to be that of the pair galaxy to which it is matched. This will allow us to see any bias associated with pair

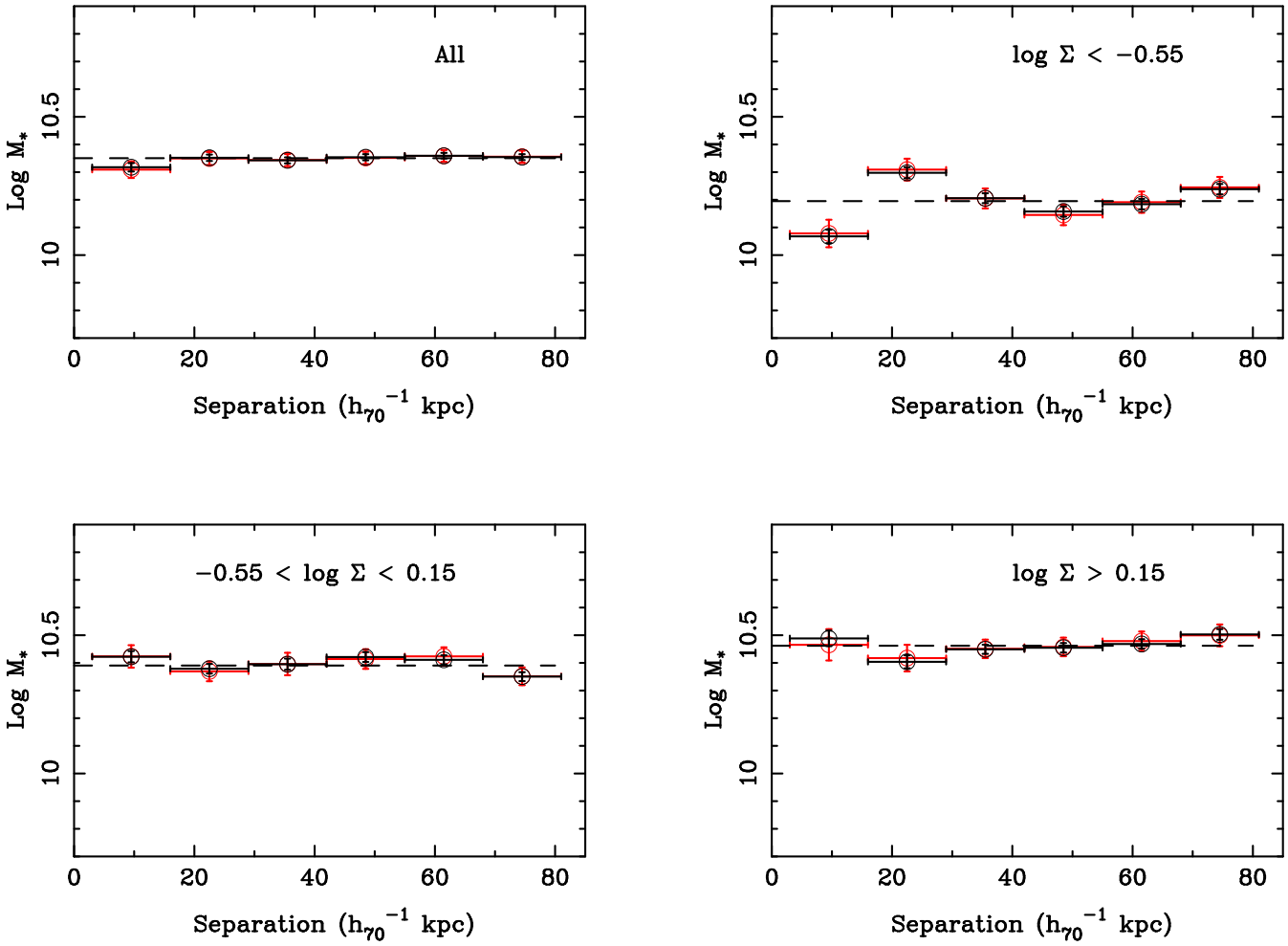

Figure 5. Log $M_\star$ for pair galaxies with $\Delta v < 200$ km s^{-1} as a function of projected separation (red points). The upper left panel shows the full sample, other panels are split by local density $\log\Sigma < -0.55$ (upper right), $-0.55 < \log\Sigma < 0.15$ (lower left) and $\log\Sigma > 0.15$ (lower right). The median value of stellar mass for the appropriate density control galaxies are shown as horizontal dashed lines. Black points show the control galaxies in projected separation bins that correspond to the pair to whch they are matched.

identification as a function of separation. Although the full pairs sample shows a 10% increase in SSFR at small projected separations ($r_p < 30\ h_{70}^{-1}$ kpc), the control galaxies matched to the closest separation pairs also exhibits a small enhancement over the median of the full control sample. This is due to the slightly lower mass of both the pairs and the control samples in the smallest r_p bin (Figure 5). However, splitting the sample into density tertiles reveals a much clearer enhancement in the SSFR at low Σ that is significant above the control out to 30 h_{70}^{-1} kpc. At intermediate densities, there is a significant enhancement in SSFR at $r_p \sim 20\ h_{70}^{-1}$ kpc, but not in the innermost bin. However, the statistics are fairly sparse at the smallest separations. The increase in SSFR at low and intermediate densities is consistent with the study of Alonso et al. (2004) who found that galaxies in both the group and field environments could experience triggered star formation in close pairs. The highest density bin shows no significant trend of enhanced SSFR relative to the control at small r_p. We conclude that only at the lowest densities is the evidence for triggered star formation robust, with a possible enhancement at intermediate densities.

3.3 Bulge fractions

A number of works have previously found that galaxies with a close companion have higher central concentrations (e.g. Nikolic et al. 2004; Li et al. 2008). Perez et al. (2009b) found that this trend is strongest at intermediate densities, although they did not investigate the dependence with projected separation. Concentration is usually defined as a ratio of the different fractional light radii (e.g. r_{50} and r_{90}). With GIM2D, a complementary metric can be used, namely the fraction of light that is fitted in the bulge relative to the total flux. An advantage of GIM2D over concentration indices is that the software properly accounts for atmospheric seeing by including the PSF in the fitting process. Simard et al. (2002) have showed that the bulge-plus-disk deconvolution is very robust against flux contributions from additional components, even when 30% of the galaxy flux is present in superposed HII regions. This is important when considering close pairs where the allocation of flux between objects is crucial. Nonetheless, it is worth highlighting the distribution of angular separations in our sample, shown in the upper left panel of Figure 2. Only 1% of our pairs sample have angular separations less than 5 arcseconds ($\sim 5\ h_{70}^{-1}$ kpc at $z = 0.05$). As discussed by Patton et al. (in prep.), galaxies with projected sep-

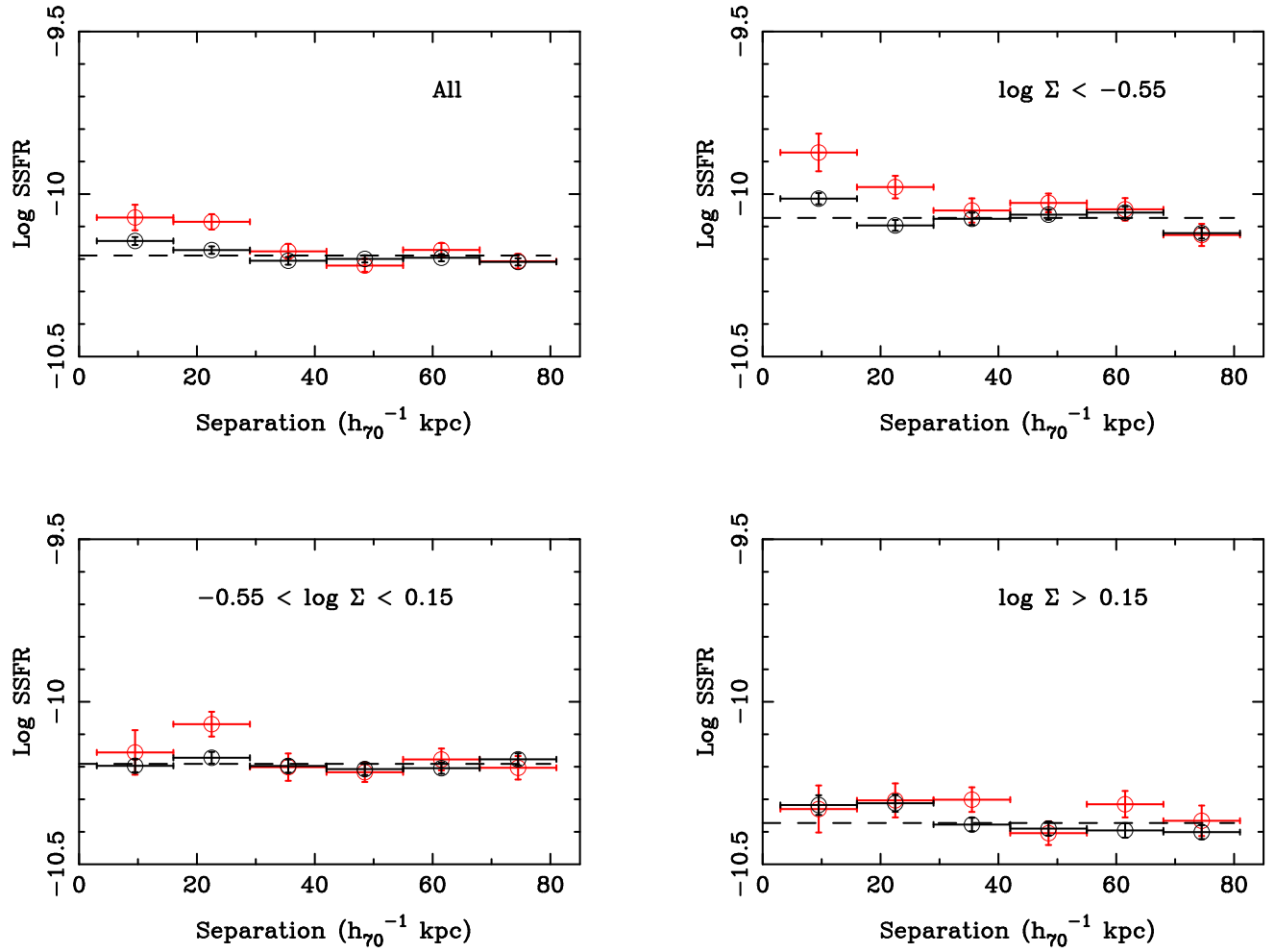

Figure 6. Specific star formation rate for pair galaxies with $\Delta v < 200$ km s^{-1} as a function of projected separation (red points). The upper left panel shows the full sample, other panels are split by local density $\log\Sigma < -0.55$ (upper right), $-0.55 < \log\Sigma < 0.15$ (lower left) and $\log\Sigma > 0.15$ (lower right). The median value of SSFR for the appropriate density control galaxies are shown as horizontal dashed lines. Black points show the control galaxies in projected separation bins that correspond to the pair to whch they are matched.

arations above 5 h_{70}^{-1} kpc are clearly distinct in the SDSS images (image mosaics are presented for close separation pairs in Patton et al.). In this and subsequent sections we show that pairs exhibit morphological trends out to projected separations of at least 20 h_{70}^{-1} kpc, i.e. at distances where there is no overlap in the SDSS images (typical half-light radii are on the order of 3 h_{70}^{-1} kpc) and GIM2D does a good job of deblending the images (Simard et al. in prep.). However, the same is not true of the public SDSS photometry, as we demonstrate below.

Before investigating the dependence of B/T in different environments, in Figure 7 we show the bulge-to-total (B/T) fractions in the *r*-band for galaxies for all values of Σ. Figure 7 ostensibly confirms previous reports of higher bulge fractions at projected separations $r_p < 30$ h_{70}^{-1} kpc (similar trends are seen in the *u* and *g*-band). However, by plotting the B/T as a function of of r_p, we see the puzzling result that the bulge fraction does not join the control galaxies at wider separations. Recall that for every pair galaxy there are four control galaxies matched in stellar mass, redshift and Σ. If there is a 'typical' B/T at a given Σ, we would expect the pair values to tend to this value at wide separations and for this value to be reflected in the control galaxies. However, Figure 7 shows that the pair galaxies have systematically higher B/T than the control even at 80 h_{70}^{-1} kpc.

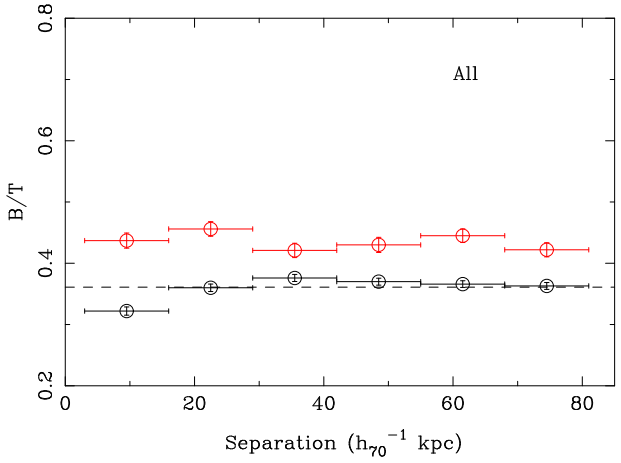

Figure 7. Bulge fractions (*r*-band) for pair galaxies (red points) with $\Delta v <$ 200 km s^{-1} in all environments. Black points are control galaxies where the separation indicates the r_p of the pair to which it is matched. The horizontal dashed line shows the median B/T values for control galaxies.

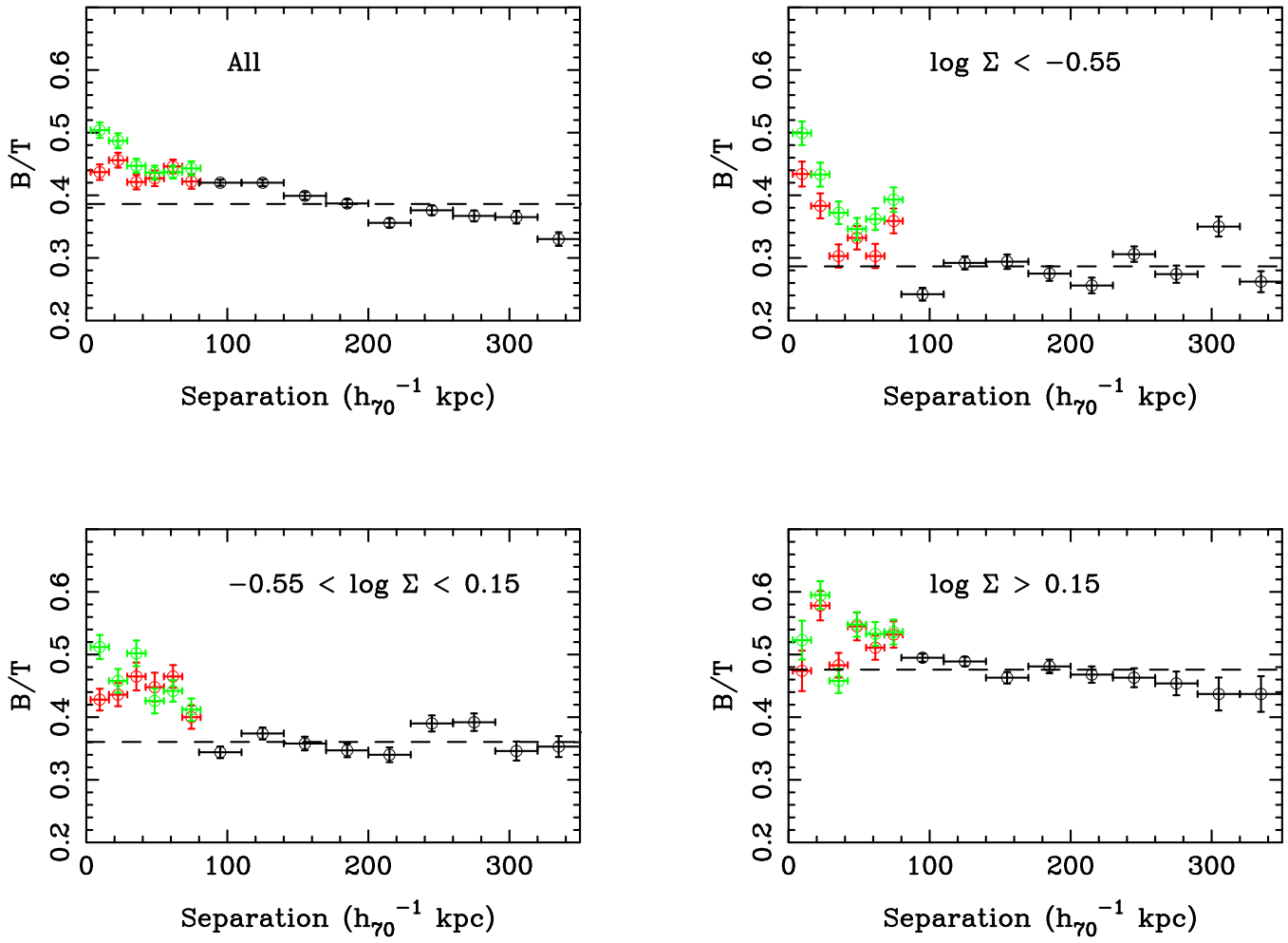

Figure 8. Bulge fractions (*r*-band) for pair galaxies (red points) with $\Delta v < 200$ km s^{-1} as a function of projected separation. Black points are control galaxies where the separation is the r_p to the nearest neighbour in the DR7. Green points also show pair galaxy B/T ratios, but derived from the original SDSS photometry where issues with the background and segmentation images can lead to fitting and photometry errors in crowded environments. The horizontal dashed line shows the median B/T values for control galaxies. The upper left panel shows the full sample, other panels are split by local density $\log\Sigma < -0.55$ (upper right), $-0.55 < \log\Sigma < 0.15$ (lower left) and $\log\Sigma > 0.15$ (lower right).

To understand the origin of the offset in B/T between pairs and control we identify the nearest galactic neighbour in the spectroscopic catalogue (DR7) for the sample of control galaxies (no companion within 80 h_{70}^{-1} kpc and 200 km s^{-1}). The DR7 is used for this test since we are not restricted by the requirement of cross-correlating with the cluster catalogue (only available for DR4). This allows us to extend the B/T versus separation plot out to larger values of r_p *using the control galaxies*, see Figure 8. Note that in Figure 8 the separation of the control galaxies is the true projected distance to its nearest neighbour, whereas in Figure 7 the separations of the control galaxies refer to the r_p of the pair galaxy to which it is matched. Figure 8 shows that (for the full sample, top left panel) there is a monotonic dependence of B/T on near neighbour distance over hundreds of kpc, an effect that is driven largely by galaxies in high density environments (lower right panel). The B/T of galaxy pairs in high densities is consistent with a continuation of the bulge fraction scaling seen out to 400 h_{70}^{-1} kpc. The trends in Figure 8 are probably manifestations of the well-known morphology-density relation (Dressler 1980) where the distance to the nearest neighbour is a coarse indicator of local environment. The control galaxies are therefore offset in Figure 7 because B/T has not reached a fiducial value at $r_p < 80\ h_{70}^{-1}$ kpc, but continues to decline, due to the dependence of B/T on both r_p and Σ. We note that this effect may contribute to the finding that pairs have a higher early type fraction (Deng et al 2008), in addition to a bias towards higher density environments (Barton et al. 2007). A simple comparison of B/T in all pair galaxies (out to 80 h_{70}^{-1} kpc) compared to the control would also indicate misleadingly high bulge-fractions, which were not associated with triggered star formation.

Figure 8 shows that the typical B/T is higher in higher density environments, as expected as the population becomes more dominated by early-type galaxies. In addition, there is a clear trend, at all values of Σ, for the bulge fractions in galaxy pairs to increase towards small separations. Taken at face value, this result indicates that galaxy-galaxy interactions increase the bulge fraction regardless of environment. However, extending our analysis to wider separations has demonstrated that local morphology-density relations may contribute to higher bulge fractions independently of ongoing interactions. At high Σ, the enhanced B/T at $r_p < 80\ h_{70}^{-1}$ kpc is actually a smooth continuation of the trend at wider separations and may therefore not be connected to the current interaction. This interpretation is consistent with our finding (Figure 6) that there

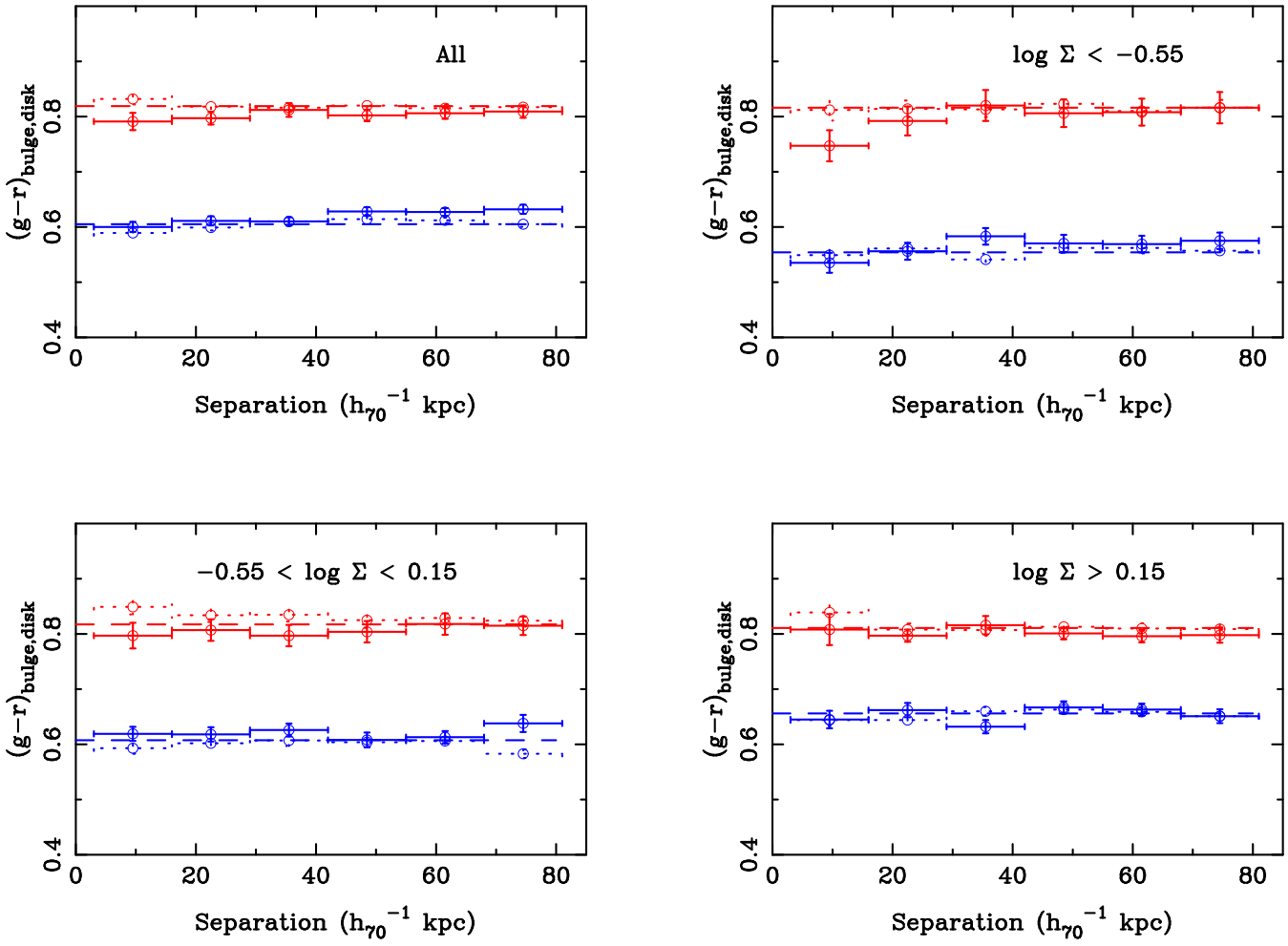

Figure 9. Median $g-r$ bulge (red) and disk (blue) colour for pair galaxies with $\Delta v < 200$ km s^{-1} as a function of projected separation. The upper left panel shows the full sample, other panels are split by local density $\log\Sigma < -0.55$ (upper right), $-0.55 < \log\Sigma < 0.15$ (lower left) and $\log\Sigma > 0.15$ (lower right). The median value of $g-r$ colours for the appropriate density control galaxies are shown as horizontal dashed lines and for individual bins in dotted lines.

is little triggered star formation in high density environments. Conversely, in the low density environments there is a striking enhancement in B/T at separations $r_p < 30\ h_{70}^{-1}$ kpc, a trend that is also seen slightly more modestly (but at wider separations) at intermediate values of Σ. Again, this agrees with the results of Figure 6 that shows that triggered star formation occurs more prolifically at lower values of Σ. Our results therefore support a picture of centrally concentrated star formation that is effective primarily in low-to-intermediate density environments.

We also demonstrate in Figure 8 the effect of crowding on the SDSS photometry. Bulge fractions derived from the original SDSS images are shown in green and fits to the improved background and segmentation images are shown in red. It can be seen that the B/T can be over-estimated at small separations when the original SDSS images and segmentation maps are used.

3.4 Bulge and disk colours

If star formation is located primarily in the galaxy centres, colour gradients might be expected to arise from a dominant blue population in the inner regions. Indeed, Barton et al. (2003) found that in their sample of 190 galaxies in pairs and compact groups many showed bluer colours in their centres. Kewley et al. (2006) measure a colour offset of the inner versus outer disk and find that this correlates with a decrease in metallicity, supporting the picture of gas inflow as a trigger.

Since GIM2D decomposes the galaxy into a bulge and disk component and calculates the relative flux in each, it is possible to examine not only the fractional distribution of the light in the two components, but also the colours of the disk and the bulge. Although $u-r$ provides one of the stronger diagnostics of star formation, there are several limitations of the u-band in the SDSS make this a less practical option. For example Baldry et al. (2005) discuss the fact that the survey limit approaches the u-band magnitude for many 'typical' galaxies and that several background issues can affect the Petrosian magnitudes. A related issue is that a non-negligibile fraction of our sample is not detected in the u-band. In Figure 9 we show the bulge and disk $g-r$ colours for pairs with $\Delta v < 200$ km s^{-1} as a function of projected separation for different cuts in Σ. The error in the bulge and disk colours is propogated from errors in the bulge and disk magnitudes and the error in the bulge fraction. Only galaxies with errors less than 0.5 mags in the bulge or disk magnitudes were considered. Figure 9 shows that the pairs sample as a whole exhibits a small bluing of the bulge, but not the disk, at small separations. When considered as a function of Σ, it is the bulges in low density environments that show a significant

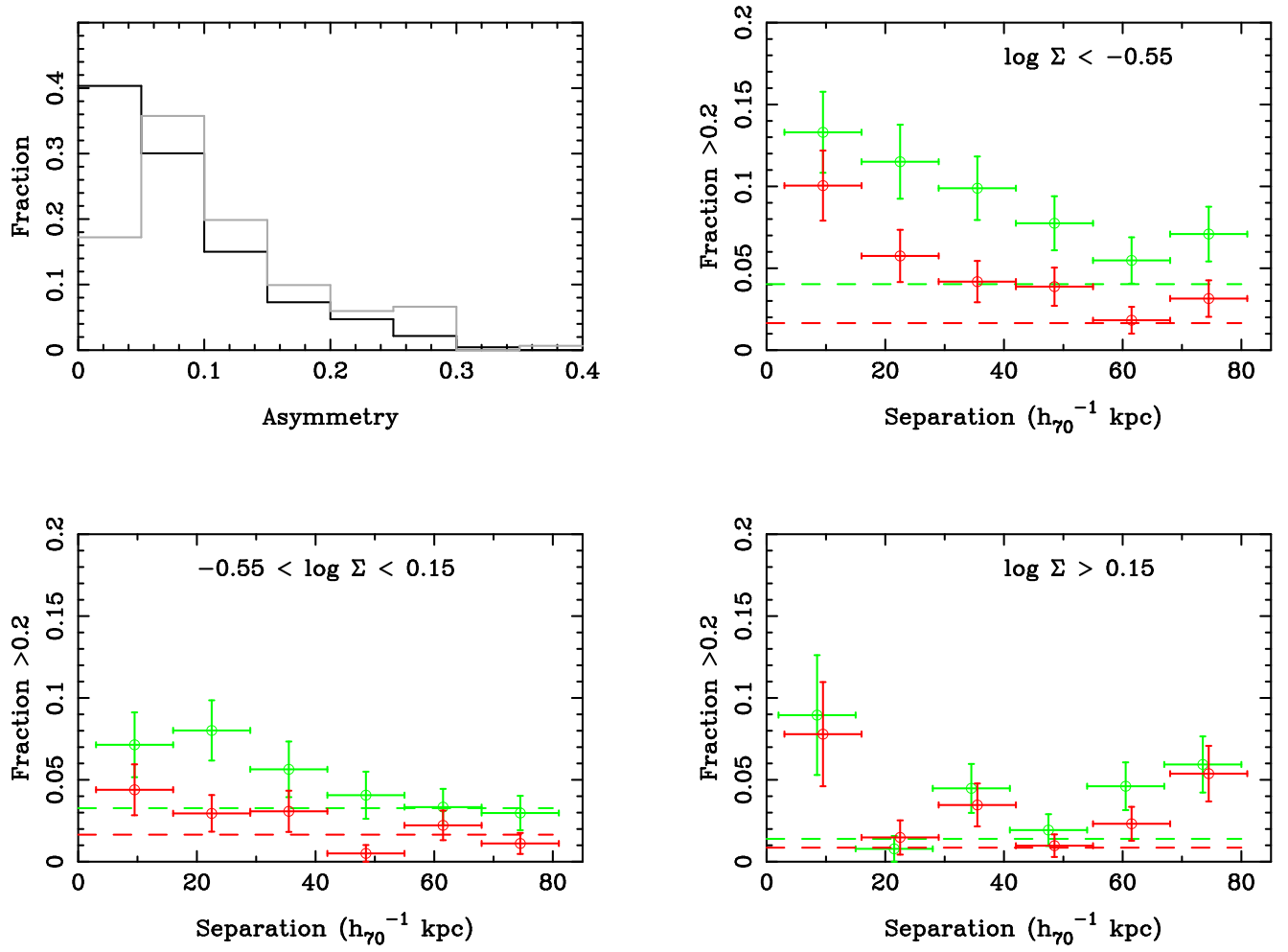

Figure 10. Top left panel: distribution of g-band asymmetries for galaxy pairs with $\Delta v < 200$ km s^{-1} and in low density environments ($\log\Sigma < -0.55$). The grey histogram is for galaxies in the innermost r_p bin ($3 < r_p < 16\ h_{70}^{-1}$ kpc) and the black histogram is for the wide separation bin with $69 < r_p < 80\ h_{70}^{-1}$ kpc. The other panels show the fraction of galaxies with a close companion within $\Delta v < 200$ km s^{-1} whose asymmetry >0.2 as a function of projected separation. Green and red points indicate asymmetry for the g and r filters respectively. Panels are split by local density: $\log\Sigma < -0.55$ (upper right), $-0.55 < \log\Sigma < 0.15$ (lower left) and $\log\Sigma > 0.15$ (lower right). The fraction of control galaxies with asymmetry > 0.2 (by Σ and filter) are shown as horizontal dashed lines. In the lower right panel, the green points have been offset horizontally by a small amount for clarity.

bluing at small separations by ~ 0.1 mag. There are no convincing colour changes in the bulge at intermediate or high densities or in the disk at any Σ. This is further evidence that galaxy-galaxy interactions are most effective at triggering central star formation in low density environments.

3.5 Asymmetry

Star formation may be expected to increase the asymmetry of galaxies, due to the clumpy nature of its distribution. Several papers have documented the increased asymmetry of galaxies in close pairs, e.g. Patton et al. (2005) and De Propris et al. (2007). However, the change in a galaxy's smoothness may depend on the competing effects of star formation and dust. Lotz et al. (2008) used simulations of galaxies with and without dust to show that extinction around star forming regions can actually smooth out the light distribution. Moreover, asymmetry in interacting galaxies can be introduced even in the absence of star formation due to the formation of tidal features. A final complication is that asymmetries may only last for a fraction of the full interaction, and the degree of asymmetry depends on internal properties (such as gas fraction) as well as the geometry of the merger (Lotz et al. 2008). The fraction of galaxies which exhibit asymmetry is therefore a conservative measure of interactions.

The top left panel of Figure 10 shows the distribution of asymmetries in the smallest separation pairs at low Σ, and a comparison of more widely separated pairs. This demonstrates that the change in asymmetry at small r_p is not simply a wholesale shift to larger values. The change is a two-fold loss of very smooth morphologies and the development of a more extended tail of high values. Therefore, we follow Patton et al. (2005) and use fraction of galaxies with asymmetries greater than a threshold value, rather than a central value estimator such as the median or mean.

The remaining three panels of Figure 10 show the fraction of galaxies with asymmetry greater than 0.2 in the g and r bands as a function of projected separation. For clarity, we do not plot the control galaxies as a function of separation, but simply their high asymmetry fraction calculated for the appropriate filter and Σ. The asymmetric fraction increases towards small separations; this is true for all environments, even though there is little evidence for strong star

formation in the high Σ sample. This indicates that the increased asymmetry is not (solely) due to clumpy star formation, since we see no other evidence for star formation at high Σ, e.g. from SSFRs or bulge colours. The asymmetries in high density environments are more likely to be associated with tidal features. Further clues to the source of the asymmetry comes from looking at the contrast between different filters. At low densities, the increase in asymmetry at small r_p is more enhanced in the *g*-band than the *r*-band, consistent with expectations from star formation. At high densities, the *g* and *r*-band show equal asymmetry enhancements, indicating that the colour of the residuals is not changing. This is expected if the asymmetry is caused by a re-distribution of the existing stellar population, e.g. through tidal disruption. Taken together, these results indicate that galaxy-galaxy interactions occur at all densities, but that triggered star formation is restricted to the lower density environments. One explanation for this result is the tendency for galaxies in high density environments to be relatively gas poor, and therefore lack the gas content to feed new star formation. We return to this suggestion in the context of other recent results in Section 5.

4 THE ENVIRONMENT OF GALAXY PAIRS: CLUSTER MEMBERSHIP.

In this section we investigate what larger structures galaxy pairs are embedded in and how this might affect interactions. Specifically, we consider more extreme structural membership, by investigating galaxy pairs located in a previously compiled cluster catalogue. The cluster catalogue is based on the compilation of von der Linden et al. (2007) who refined the C4 algorithm (Miller et al. 2005) and applied it to the DR4. The original C4 catalogue identifies galaxy overdensities in seven-dimensional position and colour space. The DR2 catalogue of Miller et al. (2005) is estimated to be 90% complete and 95% pure. In applying the C4 algorithm to the DR4, von der Linden et al. (2007) made a number of improvements, such as removing clusters with unusual velocity distributions, or the calculation of radius and velocity dispersion does not converge. Clusters without a clearly identifiable brightest cluster galaxy were also removed. The final von der Linden catalogue contains 625 clusters containing a total of 18,100 galaxies. After applying the additional criteria described in Section 2 and requiring that the galaxy is associated with a unique cluster, 14,857 galaxies remain in our cluster catalogue.

Of the 5784 galaxies in our pairs sample, 896 (15%) have been identified as a cluster galaxy in the C4 compilation. In practice, there are likely to be many pairs in clusters that do not appear in our sample due to fibre collision incompleteness. For example, 58% of galaxies in the VIVA Virgo cluster sample have a close companion within 80 kpc and 300 km s^{-1} (Chung, 2009, private communication). However, the majority of galaxies with a close companion in our SDSS-selected sample are not identified as cluster members. In Figure 11 we investigate where in the cluster the 896 pairs are located and whether or not they inhabit a particular subset of C4 clusters. The Figure shows the distribution of cluster size (R200), velocity dispersion (σ_v) and number of galaxy members for all clusters in our catalogue, and those clusters in which a close pair has been identified. Also shown is the distribution of clustercentric radii (RR200) in units of R200 for all C4 catalogue members and the 896 members with a close companion. Figure 11 shows that the clusters in which we have identified close pairs have larger mean velocity dispersions, smaller clustercentric distances,

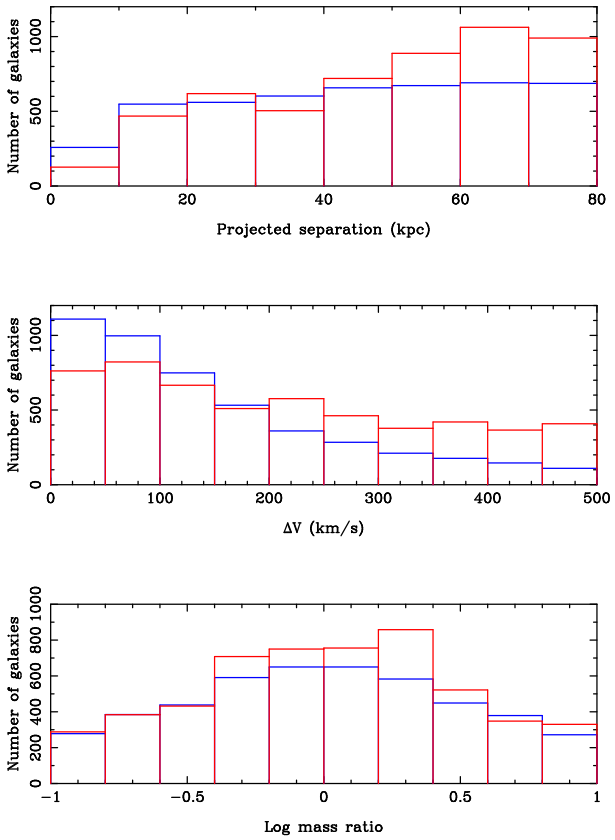

Figure 12. Histograms of pairwise properties for galaxies in clusters (red) and the field (i.e., non-clusters, blue). The cluster histogram has been scaled by a factor of 5 for presentation purposes.

R200 sizes and number of galaxy members than the full C4 sample.

In Figure 12 we show the pairwise properties of our galaxy pairs sample colour coded according to whether or not they appear in the cluster catalogue. We see a similar trend for membership classification as for environment parameterization by Σ (Figure 4), i.e. a tendency towards wider projected separations and large Δv in the clusters than the 'field' pairs. The connection between high Σ and cluster membership is demonstrated explicitly in Figure 13, where the projected densities of field and cluster pairs are plotted. 82% of pairs in clusters are in the highest density tertile ($\log\Sigma > 0.15$). However, 62% of the highest density tertile pairs are non-cluster.

4.1 Mergers in clusters

Despite the locally high densities, clusters are often considered inhospitable for galaxy mergers due to the large velocity dispersions involved. Instead, the group environment is assumed to be the prime location for mergers. For example, Wilman et al. (2009) find S0s dominate in group environments, and Just et al. (2010) find the S0 fraction evolves most strongly in intermediate velocity dispersion structures. These results imply that groups are an important location for spiral mergers, in agreement with the idea of group 'pre-processing' (e.g. McGee et al. 2009). However, there is evidence that interactions (if not mergers) do nonetheless occur in clusters. For example, Chung et al. (2007) found that 6/7 of the late-type Virgo cluster galaxies in their sample which exhibit long

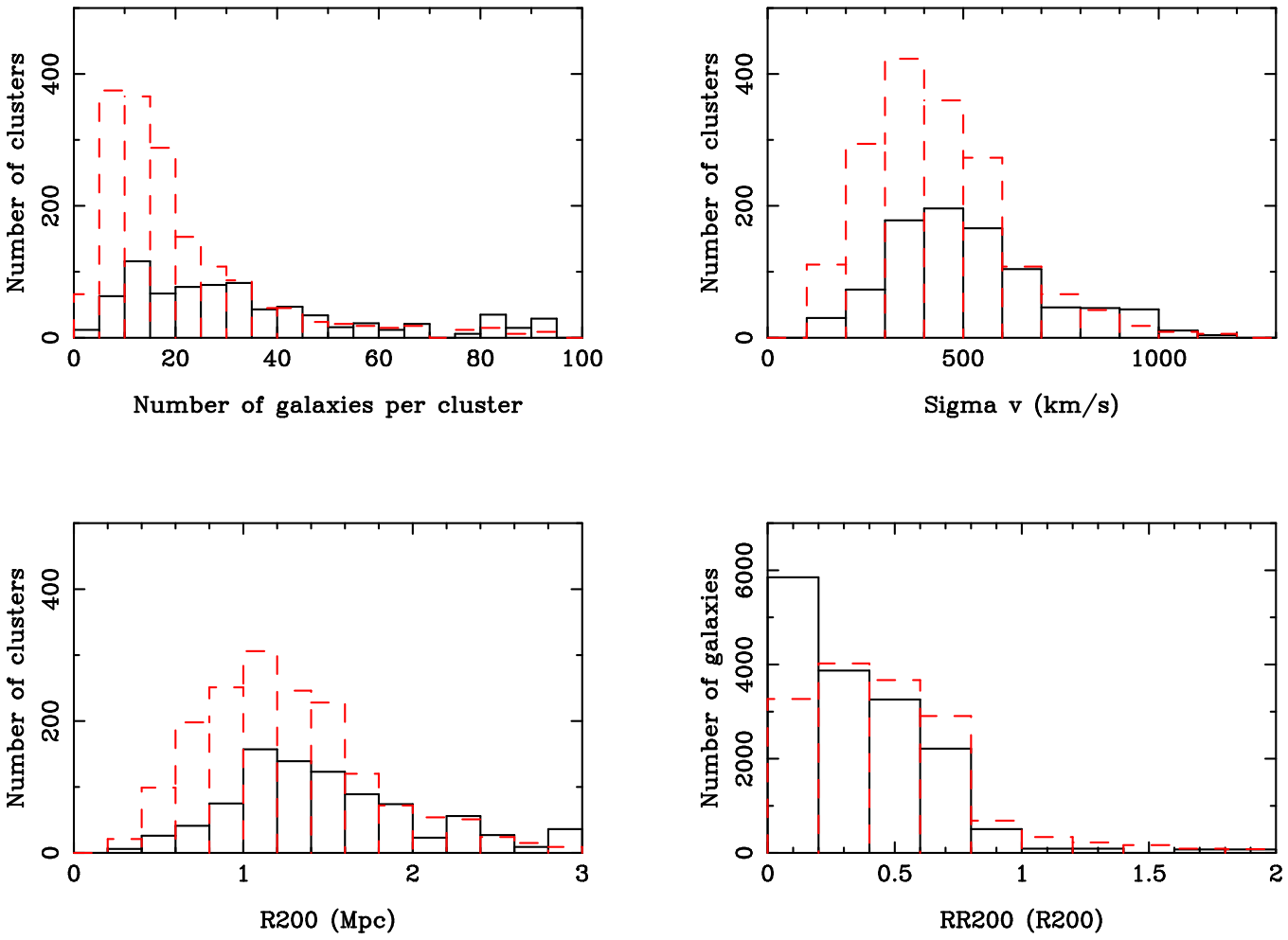

Figure 11. Histograms of cluster properties for galaxies in full C4 sample (red dashed line) and the clusters in which close pairs have been identified (solid black line). The lower right panel shows the distributions of clustercentric radii for all C4 galaxy members (red dashed histogram) and those of close pairs (solid black line). The red dashed histograms of cluster properties have been scaled up by a factor of 2 and the solid black line for the RR200 distribution of cluster pairs has been scaled up by a factor of 17 for presentation purposes.

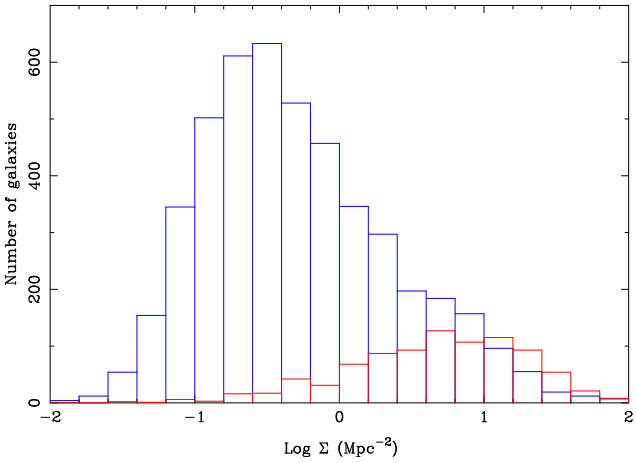

Figure 13. Distributions of projected density for pair galaxies in clusters (red), and the field (i.e., non-clusters, blue).

HI gas tails also had a close companion within 100 kpc and 100 km s^{-1}. It was suggested that tidal interactions may contribute to the efficiency of ram pressure stripping.

We investigate whether interactions are elevated in clusters by comparing the asymmetry of galaxies in close pairs (Δv < 300 km s^{-1} and r_p < 20 h_{70}^{-1} kpc) in the C4 catalogue with wide pairs (Δv > 400 km s^{-1} or r_p > 40 h_{70}^{-1} kpc) in clusters. Since we do not expect the wide pairs to be effective in galaxy-galaxy interactions, it is possible to use them as a comparison sample. Lin et al. (2010) have shown that although the galaxy pair fraction increases with density, once the higher fraction of interlopers is accounted for, the fraction of pairs that will merge actually decreases with density.

In Figure 14 we show the fraction of galaxies with *r*-band asymmetries > 0.05 as a function of clustercentric distance for the close and wide pairs. There is a mild trend towards smoother morphologies at smaller clustercentric distances in the wide pairs, as would be expected from a higher elliptical fraction in the higher local densities of the cluster core. Conversely, there is a sharp increase in the fraction of asymmetric close pairs within 0.25 R200. A 2D KS test on asymmetry and RR200 rules out the null hypothesis that the close and wide pair samples were drawn from the same distributions at 99.99% confidence. The close pairs exhibit no trend of B/T with RR200, so the high asymmetric fraction is not due to a higher spiral fraction in the inner RR200 bin. There is also no trend of SFR with RR200, indicating that the higher asymmetric frac-

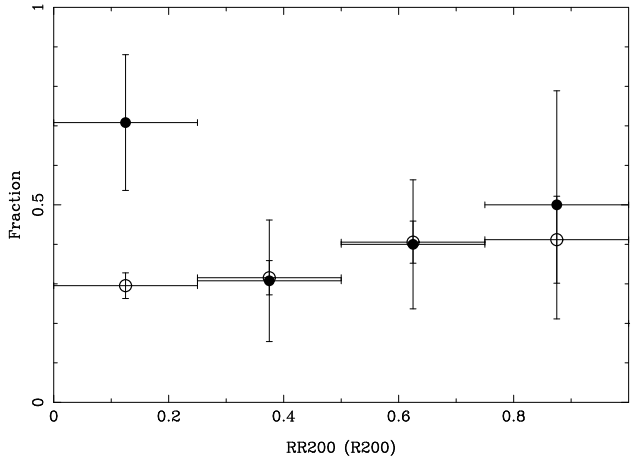

Figure 14. Fraction of galaxies with asymmetry > 0.05 in the *r*-band for close pair galaxies (Δv < 300 km s^{-1} and r_p < 20 h_{70}^{-1} kpc, solid points) and wide pairs (Δv > 400 km s^{-1} or r_p > 40 h_{70}^{-1} kpc, open points) and as a function of clustercentric distance. Only galaxy pairs that are matched in the C4 cluster catalogue are included.

tion is associated with tidal disruption rather than star formation. The local density is a strong function of clustercentric distance, with median values ranging from log $\Sigma \sim 1$ at 0.1 RR200 to log $\Sigma = -0.25$ at 0.9 RR200 for the close pairs. The high asymmetric fraction of close pairs in the inner regions of clusters shown in Figure 14 is therefore consistent with the strong increase in asymmetric fraction found at $r_p < 20\ h_{70}^{-1}$ kpc and log $\Sigma > 0.15$ in Figure 10.

5 SUMMARY & DISCUSSION

By using a sample of galaxies with a companion ($r_p < 80\ h_{70}^{-1}$ kpc, Δv < 500 km s^{-1}) selected from the SDSS DR4, combined with metrics of colour, morphology and star formation, we have examined in what environments mergers occur and what the result of the interaction is. Below we summarise our principle findings.

(i) The pairwise properties of galaxies with a close companion depend on environment. Low density environments have fractionally more pairs with low projected separations and low relative velocities than high density environments. Conversely, high density enviornoments selected either by 4+5th nearest neighbour projected density, or cluster membership are characterised by wider separations and larger values of Δv. The imposed velocity cut for a given pairs sample therefore also acts as a local density selection.

(ii) The range of stellar mass ratios does not depend on environment *for complete samples*. We select a subset of pairs with Δv < 200 km s^{-1} to study the effects of galaxy-galaxy interactions.

(iii) Galaxies in all environments, as defined by Σ, may undergo interactions if they have a close companion, as shown by increased asymmetry in the *g* and *r*-band. However, in clusters, we find evidence for galaxy-galaxy interactions (higher asymmetry) only in the cluster centre.

(iv) Triggered star formation occurs mainly in low density environments where gas fractions are expected to be typically higher. The star formation rate is also seen to increase, but to a lesser extent, in intermediate density environments. Bluer bulge $g-r$ colours indicate that the star formation occurs mainly in the central regions of galaxies.

(v) In high density environments, mergers still occur, but they are mainly without star formation. This is demonstrated by the consistent colour change in the galaxy asymmetries in the *g* and *r* filters. This is also true for pairs in clusters where we see higher asymmetries without an increase in star formation rate.

(vi) In high density environments, the bulge fraction is a monotonically increasing function of nearest neighbour separation out to at least 400 h_{70}^{-1} kpc. At lower galaxy densities, there is a clear enhancement of B/T at separations < 30 h_{70}^{-1} kpc which we interpret as the signature of the central star formation proposed above.

These results bring together three themes that have been emerging separately in the literature. First, the now well-established enhancement in star formation rate in galaxy pairs, which apparently dominates in lower density environments. Indeed, Lin et al. (2010) have shown that most 'wet' mergers (i.e. those between two gas-rich galaxies on the blue cloud) occur at low densities. Our data clearly show that this star formation occurs preferentially in the central part of the galaxy, rather than in its extended disk. Secondly, the emerging result that massive early-type galaxies are also hotbeds of merger activity. For example, Tal et al (2009) imaged a complete sample of nearby luminous ellipticals and found evidence of asymmetries in 73% of them. Despite the apparent prevalence of recent interactions, these massive galaxies showed no signs of enhanced star formation. A similar conclusion was drawn by McIntosh et al. (2008) who find no difference in colours or concentrations amongst massive major mergers in groups (although as we note above, the overall colour distribution may be relatively insensitive to modest enhancements in star formation) and Tran et al. (2008) who find only old stellar populations in their disturbed group galaxies. High density environments become systematically more dominated by masssive red galaxies (Kauffmann et al. 2004; Balogh et al. 2004; Baldry et al. 2006) and galaxy-galaxy interactions therein become more dominated by 'dry' mergers (Lin et al. 2010). This is supported by our finding that at large Σ there are enhanced colour dependent asymmetries in galaxies with small projected separations, but with no accompanying change in SFR or bulge colour. Finally, we have addressed where mergers take place. In general, mergers are considered to be rare in relaxed clusters (e.g. Makino & Hut 1997). Observationally, massive cluster galaxies show a lower incidence of interaction (through asymmetries) than galaxies in groups or the field (McIntosh et al. 2008; Liu et al 2009; Tal et al 2009). In a study of the A901/902 supercluster, Heiderman et al. (2009) identified 13 morphologically disturbed galaxies with enhanced star formation, all outside the cluster core. Our study has selected close pairs of galaxies as sites of possible mergers and is complimentary to studies which select interacting galaxies based on visible asymmetries (e.g. Lotz et al. 2010). We find evidence for tidal interactions even in the cluster core, although with no signs of associated star formation.

In summary, galaxy-galaxy interactions appear to be ubiquitous in the local universe. However, despite their ubiquity, the observational manifestation of the interaction, such as triggered star formation, colour changes and tidal disruption, depends markedly on environment.

ACKNOWLEDGMENTS

We are grateful to Anja von der Linden and the MPA/JHU group for access to their data products and catalogues (maintained by Jarle Brinchmann at http://www.mpa-garching.mpg.de/SDSS/). Aeree Chung generously shared results of the VIVA survey in advance

of publication. Thanks to Josefa Perez for comments on a previous draft. SLE and DRP acknowledge the receipt of NSERC Discovery grants which funded this research.

REFERENCES

Alonso, M. S., Tissera, P. B., Coldwell, G., Lambas, D. G., 2004, MNRAS, 352, 1081
Alonso, M. S., Lambas, D. G., Tissera, P. B., Coldwell, G., 2006, MNRAS, 367, 1029
Baldry, I. K., Balogh, M. L., Bower, R. G., Glazebrook, K., Nichol, R. C., Bamford, S. P., Budavari, T., 2006, MNRAS, 373, 469
Baldry, I. K., Glazebrook, K., Budavri, T., Eisenstein, D. J., Annis, J., Bahcall, N. A., Blanton, M. R., Brinkmann, J., Csabai, I., Heckman, T. M., Lin, H., Loveday, J., Nichol, R. C., Schneider, D. P., 2005, MNRAS, 358, 441
Balogh, M. L., Baldry, I. K., Nichol, R., Miller, C., Bower, R., Glazebrook, K., 2004, ApJ, 615, L101
Bamford, S. P., et al., 2009, MNRAS, 393, 1324
Barton, E. J., Geller, M. J., & Kenyon, S. J., 2000, ApJ, 530, 660
Barton, E. J., Geller, M. J., & Kenyon, S. J., 2003, ApJ, 582, 668
Barton, E. J., Arnold, J. A., Zentner, A. R., Bullock, J. S., Wechsler, R. H., 2007, ApJ, 671, 1538
Basu-Zych, A. R., 2009, ApJ, 699, 1307
Bekki, K., Noguchi, M., 1994, A&A, 290, 7
Bekki, K., Shioya, Y., 2001, ApJS, 134, 241
Bekki, K., Shioya, Y., & Whiting, M., 2006, MNRAS, 371, 805
Bergvall, N., Laurikainen, E., Aalto, S., 2003, A&A, 405, 31
Blanton, M. R., & Berlind. A. A., 2007, ApJ, 664, 791
Blanton, M. R., & Roweis, S., 2007, AJ, 133, 734
Bridge, C. R., et al., 2007, ApJ, 659, 931
Brasseur, C. M., McConnachie, A. W., Ellison, S. L., Patton, D., 2008, MNRAS, 392, 1141
Brinchmann, J., Charlot, S., White, S. D. M., Tremonti, C., Kauffmann, G., Heckman, T., Brinkmann, J.,2004, MNRAS, 351, 1151
Chung, A., van Gorkom, J. H., Kenney, J. D. P., Vollmer, B., 2007, ApJ, 659, L115
Cox, T. J., Jonsson, P., Somerville, R. S., Primack, J. R., Dekel, A., MNRAS, 2008, 384, 386
Darg, D. W., et al., 2010, MNRAS, 401, 1552
De Propris, R., Conselice, C. J., Liske, J., Driver, S. P., Patton, D. R., Graham, A. W., Allen, P. D., 2007, ApJ, 666, 212
Deng, X.-F. He, J.-Z., Wen, X.-Q., Tang, X.-X., 2009, MNRAS, 395, L90
Deng, X-F., He, J-Z., Jiang, P., Song, J., Tang, X-X., 2008, ApJ, 677, 1040
Di Matteo, P., Combes, F., Melchior, A.-L., Semelin, B., 2007, A&A, 468, 61
Donzelli, C. J., & Pastoriza, M. G., 1997, ApJS, 111, 181
Dressler, A., 1980, ApJ, 236, 351
Ellison, S. L., Patton, D. R., Simard, L., McConnachie, A. W., 2008 AJ, 135, 1877
Ellison, S. L., Simard, L., Cowan, N. Baldry, I. K., Patton, D. R., McConnachie, A. W., 2009, MNRAS, 396, 1257
Geller, M. J., Kenyon, S. J., Barton, E. J., Jarrett, T. H., Kewley, L. J., 2006, AJ, 132, 2243
Gomez, P., et al., 2003, ApJ, 584, 210
Heiderman, A., et al., 2009, ApJ, 705, 1433
Holmberg, E., 1958, Medd. Lund. Astron. Obs. Ser., 2, 136
Jonsson, P., Cox, T. J., Primack, J. R., Somerville, R. S., 2006, ApJ, 637, 255
Just, D. W., Zaritsky, D., Sand, D. J., Desai, V., Rudnick, Gregory, 2010, ApJ, 711, 192
Kannappan, S. J., Jansen, R. A., Barton, E. J., 2004, AJ, 127, 1371
Kauffmann, G., et al., 2003, MNRAS, 341, 33
Kauffmann, G., White, S. D. M., Heckman, T. M., Menard, B., Brinchmann, J., Charlot, S., Tremonti, C., Brinkmann, J., 2004, MNRAS, 353, 713
Kennicutt, R. C., Jr., Roettiger, K. A., Keel, W. C., van der Hulst, J. M., Hummel, E., 1987, AJ, 93, 1011
Kewley, L. J., Geller, M. J., Barton, E. J., 2006, AJ, 131, 2004
Knapen, J. H., & James, P. A., 2009, ApJ, 698, 1437
Lambas, D. G., Tissera, P. B., Alonso, M. S., Coldwell, G., 2003, MNRAS, 346, 1189
Lewis, I., et al. 2002, MNRAS, 334, 673
Li, C., Kauffmann, G., Heckman, T. M., Jing, Y. P., White, S. D. M., 2008, MNRAS, 385, 1903
Lin, L., et al. 2007, ApJ, 660, L51
Lin, L., et al. 2010, ApJ, arXiv:1001.4560
Lotz, J. M., Jonsson, P., Cox, T. J., Primack, J. R., 2008, MNRAS, 391, 1137
Lotz, J. M., Jonsson, P., Cox, T. J., Primack, J. R., 2010, MNRAS, in press
Liu, F. S., Mao, Shude, Deng, Z. G., Xia, X. Y., Wen, Z. L. 2009, MNRAS, 396, 2003
Luo, Z.-J. Shu, C.-G., Huang, J.-S., 2007, PASJ, 59, 541
Ma, C. J., & Ebeling, H., American Astronomical Society, AAS Meeting #213, #362.01; Bulletin of the American Astronomical Society, Vol. 41, p.512
Makino, J., & Hut, P., 1997, ApJ, 481, 83
Masjedi, M., et al., 2006, ApJ, 644, 54
McConnachie, A. W., Ellison, S. L., Patton, D., 2008, MNRAS, 387, 1281
McConnachie, A. W., Patton, D., Ellison, S. L., Simard, L., 2009, MNRAS, 395, 255
McGee, S. L., Balogh, M. L., Bower, R. G., Font, A. S., McCarthy, I. G., 2009, MNRAS, 400, 937
McIntosh, D. H., Guo, Y., Hertzberg, J., Katz, N., Mo, H. J., van den Bosch, F. C., Yang, X., 2008, MNRAS, 388, 1537
Mihos, C., & Hernquist, L., 1994, ApJ, 425, L13
Mihos, C., & Hernquist, L., 1996, ApJ, 464, 641
Miller, C. J., et al., 2005, AJ, 130, 968
Nikolic, B., Cullen, H., Alexander, P., 2004, MNRAS, 355, 874
Park, C., Choi, Y.-Y., Vogeley, M. S., Gott, J. R., Blanton, M. R., 2007, ApJ, 658, 898
Park, C., & Choi, Y.-Y., 2009, ApJ, 691, 1828
Patton, D. R., & Atfield, J. E., 2008, ApJ, 685, 235
Patton, D. R., Grant, J. K., Simard, L., Pritchet, C. J., Carlberg, R. G., Borne, K. D., 2005, AJ, 130, 2043
Perez, M. J., Tissera, P. B., Blaizot, J., 2009a, MNRAS, 397, 748
Perez, M. J., Tissera, P. B., Lambas, D. G., Scannapieco, C., 2006, A&A, 449, 23
Perez, M. J., Tissera, P. B., Padilla, N., Alonso, M. S., Lambas, D. G., 2009b, MNRAS, 399, 1157
Poggianti, B. M., et al., 2009, ApJ, 693, 112
Postman, M., & Geller, M. J., 1984, ApJ, 281, 95
Robaina, A., et al., 2009, ApJ, 704, 324
Rogers, B., Ferreras, I., Kaviraj, S., Pasquali, A., Sarzi, M., 2009, MNRAS, 399, 2172
Skibba, R. A., et al., 2009, MNRAS, 399, 966
Simard, L., Willmer, C. N. A., Vogt, N. P., Sarajedini, V. L., Phillips, A. C., Weiner, B. J., Koo, D. C., Im, M., Illingworth, G. D., Faber, S. M., 2002, ApJS, 142, 1
Soto, K. T., & Martin C. L., 2009, arXiv:0909.2050
Tal, T., van Dokkum, P. G., Nelan, J., Bezanson, R., 2009, AJ, 138, 1417
Tran, K-V., Moustakas, J., Gonzalez, A. H., Bai, L., Zaritsky, D. Kautsch, S. J., ApJ, 683, L17
von der Linden, A., Best, P. N., Kauffmann, G., White, S. D. M., 2007, MNRAS, 379, 867
Weinmann, S. M., van den Bosch, F. C., Yang, X., Mo, H. J., 2006, MNRAS, 366, 2
Woods, D. F., Geller, M. J., Barton, E. J., 2006, AJ, 132, 197
Woods, D. F., Geller, M. J., 2007, AJ, 134, 527
Zhang, W., Li, C., Kauffmann, G., Zou, H., Catinella, B., Shen, S., Guo, Q., Chang, R., 2009, MNRAS, 397, 1243